ELSEVIER

Probabilistic Engineering Mechanics 16 (2001) 177–191

PROBABILISTIC ENGINEERING MECHANICS

www.elsevier.com/locate/probengmech

Site-dependent design input ground motion estimations for the Taipei area: a probabilistic approach

V. Sokolov[a,1,*], C.-H. Loh[a], K.-L. Wen[b,2]

[a]*National Center for Research on Earthquake Engineering, 200, Sec. 3, Hsinhai Road, Taipei, Taiwan, ROC*
[b]*Institute of Applied Geology, National Central University, 38, Wu-chuan Li, Chumg-li, Taiwan, ROC*

Accepted 24 October 2000

Abstract

Design seismic forces depend on the peak ground acceleration (PGA) and on the shape of design spectrum curves dictated in building codes. At present there is no doubt that it is necessary to construct so-called "site and region-specific" design input ground motions reflecting influence from different magnitude events at different distances that may occur during a specified time period. A unified approach to ground motion parameters estimation is described. A collection of ground motion recordings of small to moderate ($3.0–3.5 \leq M_L \leq 6.5$) earthquakes obtained during the execution of the Taiwan Strong Motion Instrumentation Program (TSMIP) since 1991 was used to study source scaling model, attenuation relations and site effects in Taiwan region. A stochastic simulation technique was applied to predict PGA and response spectra for the Taipei basin. "Site and region-dependent" uniform hazard response spectra were estimated for various geological conditions in the Taipei basin using a technique of probabilistic seismic hazard analysis.

Keywords: Strong ground motion; Site response; Seismic hazard assessment

1. Introduction

The design of buildings and structures in earthquake-prone regions must be based on information relating to expected seismic effect expressed in terms of time domain quantities (maximum amplitudes of ground motion, periods and duration) and spectral quantities (Fourier amplitude spectra and response spectra). Design of some critical facilities also requires the time function of ground acceleration. Estimation of the time domain and spectral parameters of ground motion are obtained either by empirical relations that connect these to earthquake magnitude, distance and local soil conditions (source scaling and attenuation relations) or by means of mathematical modeling. At present, there is no doubt that these relations are different for different seismic regions; "region and site-specific" models should be developed on the basis of available strong ground motion records. The accuracy and reliability of the source scaling and attenuation models depend entirely on the quality and amount of empirical data used for the evaluation of the models. Therefore, the large number of ground motion acceleration recordings obtained during the execution of the Taiwan Strong Motion Instrumentation Program (TSMIP) since 1991 [1] provide a unique opportunity to study source scaling and attenuation relations for a wide range of earthquake magnitudes and distances in the Taiwan region.

Recent needs of earthquake engineering require local site effects to be included into seismic hazard estimation. The characteristics of site response depend on input motion characteristics (amplitude, frequency content, etc.) and therefore, on the source and propagation path features [2–4]. The need for realistic representation of source, path and site effects requires a model that considers these three factors separately. The characteristics of site response should reflect the variability of the response depending on the source parameters and propagation path peculiarities. In addition, it should be possible to use them in conjunction with an accepted strong ground motion attenuation model to produce realistic estimates.

A dense strong motion network in the Taipei area allows us to study site response parameters of the Taipei sediment-filled basin. The results of the previous researches of earthquake ground motion peculiarities in the Taipei basin [1,5–7] showed that, although the basin is not a large area, it reveals a large variation in ground motion characteristics (amplitude

* Corresponding author. Tel.: +886-2-2632-6607; fax: +886-2-2732-2223.

E-mail addresses: vova@ncree.gov.tw (V. Sokolov), lohc@ncree.gov.tw (C.-H. Loh), wenkl@eqm.gep.ncu.edu.tw (K.-L. Wen).

[1] Geophysical Institute, Karlsruhe University, Hertzstr. 16, Karlsruhe 76187, Germany. Fax: +49-721-71173.

[2] Fax: +886-3-4263127.

0266-8920/01/$ - see front matter
PII: S0266-8920(00)00021-7

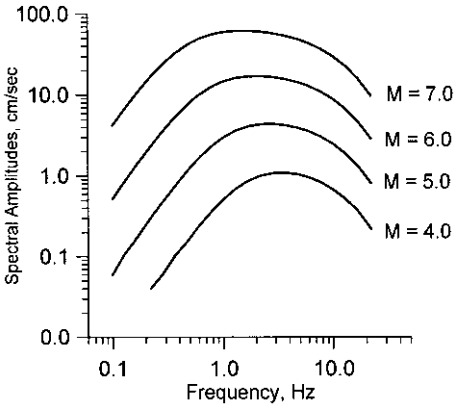

Fig. 1. Theoretical ω-square spectra of ground acceleration for the Taiwan region, Very Hard Rock (VHR) site, distance $R = 10$ km.

and shape of site amplification functions, dominant frequencies, response spectra, etc.). These characteristics depend on the geotechnical properties at the site, location of the station and on the parameters of the earthquakes. Therefore one single building code design spectrum provided for the Taipei basin [8] is not adequate for the whole basin area. Instead of standard design parameters, it is necessary to construct site-specific parameters reflecting the influence from different magnitude events at different distances that may occur with a certain probability during the lifetime of the construction. Probabilistic seismic hazard analysis (PSHA) is an efficient tool for this purpose, because it produces integrated description of the influence from all damaging events at all possible locations with respect to a specific case. It is common practice to estimate so-called uniform hazard response spectra (UHS), which represent uniform probabilities of spectral amplitude exceedance during a specified time period, and the design spectra are constructed on the basis of UHS.

The goal of the paper is to present the procedure and the results of the probabilistic estimation of "site and region-dependent" design input ground motion parameters for the Taiwan area and, particularly, for the Taipei basin, which can be used for the improvement of the building code provisions. The empirical models for ground motion parameters (regional source scaling and attenuation models, site response amplification functions), which provide a basis for quantitative seismic hazard estimation, are shortly described.

2. Source scaling and attenuation models

A collection of ground motion recordings (1380 acceleration records) of small to moderate ($4.5 \le M_L \le 6.5$) earthquakes obtained at distances up to 200 km was used to study source scaling model and attenuation relations for the Taiwan region [9]. The general model of radiated spectra, describing the Fourier acceleration spectrum A at frequency f, can be expressed as follows [10]

$$A(f) = (2\pi f)^2 CS(f)D(R,f)I(f) \tag{1}$$

where C is the scaling factor; $S(f)$ is the source spectrum; $D(R,f)$ is the diminition function and $I(f)$ represents frequency-dependent site response. The scaling factor is given by

$$C = (\langle R_{\theta\phi}\rangle FV)/(4\pi\rho\beta^3 R^b) \tag{2}$$

where $\langle R_{\theta\phi}\rangle$ is the radiation coefficient, F is the free surface amplification, V represents the partitions of the vector into horizontal components, ρ and β are, respectively, the density and shear velocity in the source region and R is the hypocentral distance.

A commonly used source function $S(f)$ in the Brune's model [11] is

$$S(f) = M_0/[1 + (f/f_0)^2] \tag{3}$$

For the Brune's model, the source acceleration spectrum at low frequencies increases as f^2 and approaches a value determined by f_0 (corner frequency) and M_0 at frequencies $f > f_0$. The value of f_0 can be found from the relation $f_0 = 4.9 \times 10^6 \beta(\Delta\sigma/M_0)^{1/3}$. Here $\Delta\sigma$ is the stress parameter in bars, M_0 is the seismic moment in dyne centimeters and β is in kilometers per second. The level of the spectrum remains approximately constant for frequencies above f_0 until the cut-off frequency f_{max} is approached. The amplitude of the spectrum decays rapidly at frequencies above f_{max}.

The function $D(R,f)$ accounts for frequency-dependent attenuation that modifies the spectral shape. It depends on the hypocentral distance (R), regional crustal material properties, the frequency-dependent regional quality factor Q and f_{max}. These effects are represented by the equation

$$D(R,f) = \exp[-\pi f R/Q(f)\beta]P(f,f_{max}) \tag{4}$$

where $P(f,f_{max})$ is a high-cut filter. We used the P-filter proposed by Anderson and Hough [12]

$$P(f) = \exp(-\pi\kappa f) \tag{5}$$

The results of our study reveal that the acceleration spectra of the most significant part of the records, starting from S-wave arrival, for hypothetical very hard rock (VHR) sites ($\rho = 2.8$ g/cm^3, $\beta = 3.8$ km/s, $I(f) = 1$) in the Taiwan area can be modeled accurately by the single-corner frequency Brune ω^{-2} source model with magnitude-dependent stress parameter $\Delta\sigma$. The parameters of the model should be determined using recently proposed regional relationships, firstly, between seismic moment (M_0) and magnitude (M_L) [13]

$$\log_{10} M_0 = 19.043 + 0.914 M_L \tag{6}$$

and, secondly, between $\Delta\sigma$ and M_0 [14]

$$\log_{10} \Delta\sigma = -3.3976 + 0.2292 \log_{10} M_0 \pm 0.6177 \tag{7}$$

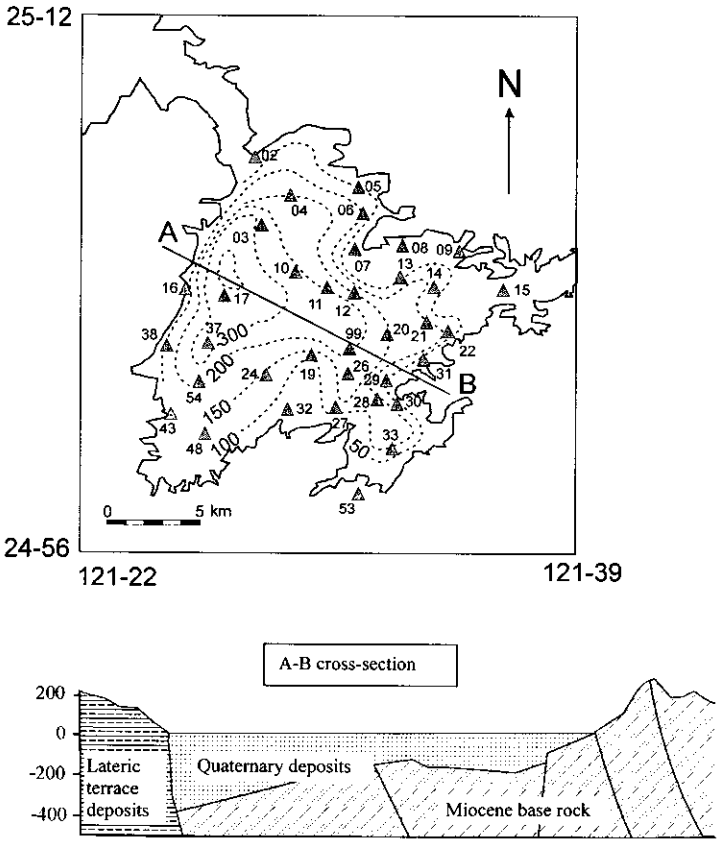

Fig. 2. Map of the Taipei basin and location of the TSMIP network stations (triangles) recordings of which were used for site response study. The numbers indicate the station codes. The dotted contours show the depth in meters to the base rock surface.

Frequency-dependent attenuation of spectral amplitudes with distance may be described using quality factor $Q = 225f^{1.1}$ for deep (depth greater than 35 km) earthquakes and $Q = 125f^{0.8}$ for shallow earthquakes; a kappa filter ($\kappa = 0.03$) may be used to modify the spectral shape. The parameter κ, which usually is considered to be region and site dependent, vary significantly even within the same region [15–17]. For example, the value of 0.035 was used by Boore and Joyner for hard rock sites in California [16]. Fig. 1 shows the examples of the VHR spectra for different magnitudes.

When considering geometrical spreading in the form $1/R^b$ (Eq. (2)), attenuation of the direct waves is described using $b = 1.0$ for $R_1 < 50$ km; for transition zone where direct wave is joined by postcritical reflections from mid-crustal interfaces and the Moho-discontinuity ($50 < R_2 <$ 150–170 km) $b = 0.0$, and attenuation of multiply reflected and refracted S-waves is described by $b = 0.5$ for $R_3 >$ 170 km. The obtained source scaling and attenuation models allow a satisfactory prediction of the peak ground acceleration (PGA) for rock sites and, combining with generalized soil amplification curves, for soil sites, for magnitudes $4.5 \leq M_L \leq 6.5$ and distances up to about 200 km in the Taiwan region [9]. Standard deviation of the residuals between the observed and calculated peak amplitudes of ground acceleration does not exceed 0.3 log units.

3. Local site response

The source scaling and attenuation models have been used for estimation of site response characteristics in terms of frequency-dependent amplification (spectral ratios) in the Taipei basin [18]. The approach consisted of calculating spectral ratios between spectra of actual earthquake records (horizontal components) and those modeled for a hypothetical VHR site. Actually, these spectral ratios reflect the difference between idealized source scaling, attenuation models and real recordings. Besides local site response, the spectral ratios include the effects of source rupture peculiarities and inhomogeneous propagation path. The variability of spectral ratios due to uncertainties introduced by source and propagation path effects and variability in the site response itself, may be described in terms of random variable characteristics and further used, together with source scaling and attenuation models, when estimating seismic hazards. The analysis of spectral amplification functions obtained by this approach in the Caucasus area [19] showed that the estimations are consistent with available

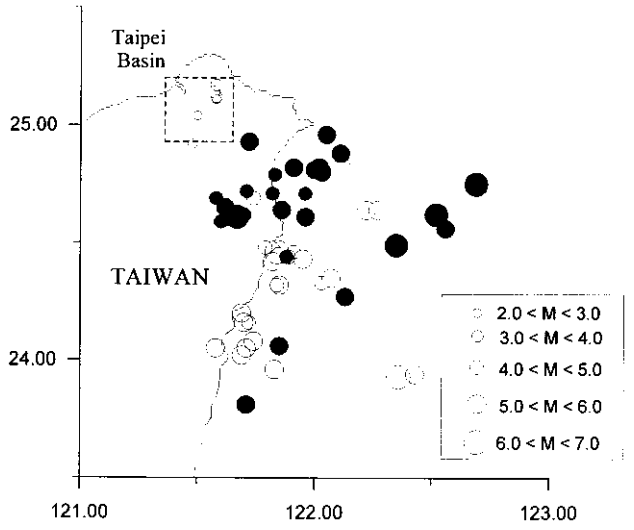

Fig. 3. Distribution of epicenters of the earthquakes recordings used in this study. Open circles indicate shallow earthquakes (hypocentral depth of which were less than 35 km), and shaded circles indicate deep events.

geotechnical data (for example, thickness of soil deposits) and produce reliable prediction of ground motion parameters.

The advantages to this technique are as follows. In the traditional spectral ratio method, the choice of reference site may be very difficult: the reference site should be located on a hard rock outcrop not far from the sedimentary site, and it should provide records of almost every earthquake. The seismic network in the Taipei basin, despite a large number of the stations, could not provide a single station which could be accepted, undoubtedly, as "hard-rock reference" station. The tightly built Taipei valley is surrounded by hills formed by weathered sandstones and shales. The stations outside the valley are located on the hill slopes or in the narrow canyons on shallow soft alluvium and reveal high resonance peaks in the spectra of the records. In the previous research the site response was studied with respect to the TAP16 site, which is near the edge of the basin [7] or the mean spectrum averaged from all records of a single earthquake [6]. In this study we used modeled VHR spectrum as a reference spectrum, and the approach makes it possible to analyze all records. The site/bedrock spectral ratio (SBSR) function reflects an intrinsic variability in the site response itself (by virtue of different incidence angles, back-azimuths, etc.) and the source and path effects. The results in conjunction with the same "hard rock" spectral model used can then be incorporated into "site-dependent" seismic hazard assessment.

The Taipei basin is a triangular alluvium structure, and the area (about 240 km^2) is almost flat with an altitude of less than 20 m. The geological structure inside the basin consists of Quaternary layers above a Tertiary base rock. Maximum thickness of the Quaternary deposits is about of 400 m in the northwestern part of the basin. The average values of S-wave velocity change from 170 m/s for the upper Quaternary layer, up to 650 m/s for the deepest layer, and the base rock is characterized by the average S-velocity of 1200 m/s. Fig. 2 shows a scheme of the Taipei basin and stations of the Taipei Strong Motion Observation Network whose recordings were used. The data set used for the site response study included recordings of 66 earthquakes of $M = 2.6$–6.5, with hypocentral depth varying from 1 to 118 km and hypocentral distances of up to

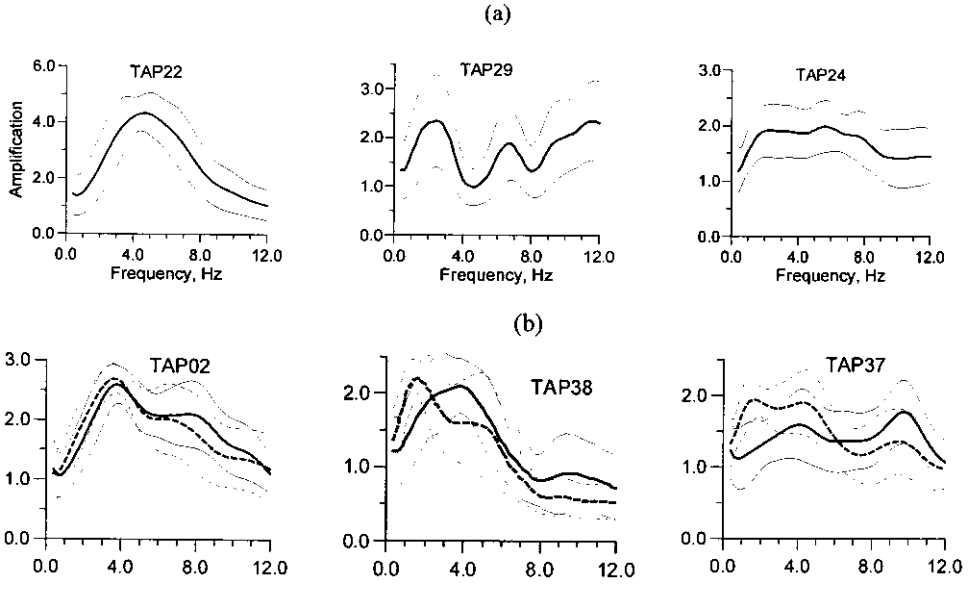

Fig. 4. Characteristics of the site amplification (examples) in the Taipei basin: (a) the amplification functions showing three categories of the site response: single resonance peak, multiple well defined resonance and broadband amplification. The thick solid lines represent mean-amplification values; the thin solid lines show ±1 standard deviation; and (b) comparison of the site response characteristics which were determined for deep (solid lines) and shallow (dashed lines) earthquakes. The thick lines represent mean-amplification values; the thin lines show ±1 standard deviation limits.

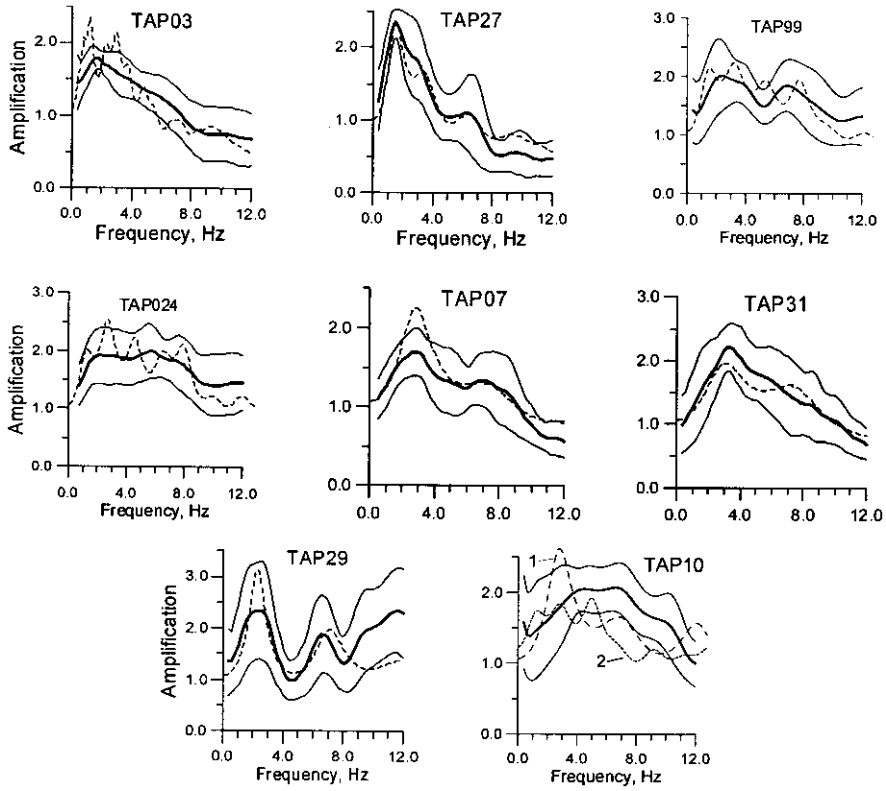

Fig. 5. Comparison between the empirical spectral ratios (solid lines; the thick line shows mean-amplitude values and the thin lines show ±1 standard deviation limits) and theoretical spectral ratios (dashed lines, the average curve for SH- and SV-waves) which were calculated using 1D models. Theoretical spectral ratios for station TAP10: 1 — the model which describes the whole Quaternary deposits (five layers); 2 — the model which describes the upper formation (three layers).

150 km, obtained at 35 stations located within the Taipei basin. Source parameters of these events are determined by the local seismic network of the Central Weather Bureau, Taiwan, and Fig. 3 shows the distribution of the epicenters.

The SBSR functions were obtained by dividing the actual smoothed spectrum by the modeled one. Processing of the records consisted of visual inspection of every accelerogram, selection of the significant part of the record starting from S-wave arrival and the computation of Fourier amplitude spectra of the horizontal components using a 10% cosine window. The spectra were smoothed using a three-point running Hanning average filter (20 consecutive smoothings were applied for raw spectra to reveal gross features of site amplification). The signal-to-noise ratio allows us to analyze the spectra at frequencies from 0.8–0.6 to 12–14 Hz. The detailed description of the procedure may be found in Ref. [18].

Depending on the shape of the mean-amplitude spectral ratios, the sites may be divided into three categories: (1) sites that are characterized by a single prominent peak for the amplification within a relatively narrow frequency band; (2) multiple, but well-defined resonances; and (3) broadband amplification. The first category, in turn, may be divided into two subcategories: (1a) the fundamental response frequency does not depend on the earthquake depth; and (1b) the resonance frequencies are different for deep and shallow events. The examples of the site amplification characteristics are shown in Fig. 4. On the one hand, it is possible to conclude that the type of amplification relates to the site geology. Resonance at a single frequency occurs when there is a uniform well-defined layer over the bedrock, and the influence of other layers is negligible. Multiple resonances are caused by a small number of well-defined layers, and broadband amplification may occur when there is a gradual increase of shear wave velocity with the depth. On the other hand, uneven basement topography and complex local structure may also produce additional resonance peaks and be a source of considerable variability in the spectral ratios.

To verify the ability of the applied method to represent the amplitude and frequency dependence of the site response, we used a simple 1D technique which allows us to calculate the theoretical spectral amplification of a multilayered soil column overlying the rigid half-space for SH- and SV-waves approaching the bottom of the soil with arbitrary angles of incidence. Theoretical spectral ratios were calculated for horizontal components of motion for SH- and SV-waves using different angles of incidence. Actually, the angles for different S-wave portions may vary significantly depending on the peculiarities of the earthquake source and propagation path. Fig. 5 shows a comparison between theoretical spectral ratios which were

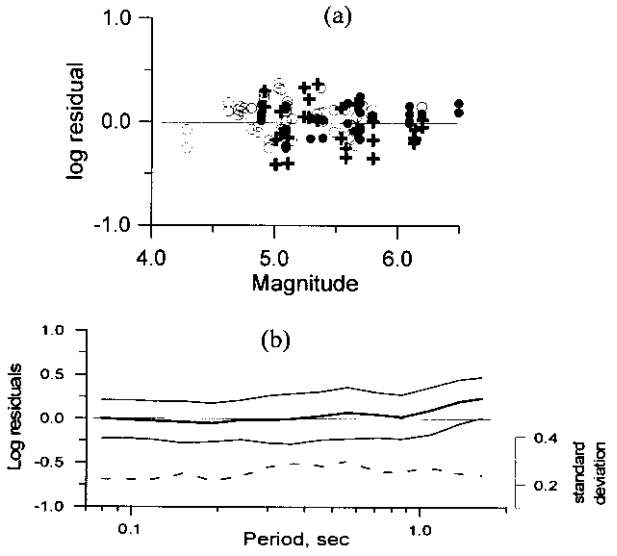

Fig. 6. Statistical characteristics of the residuals between observed and modeled ground motion parameters: (a) peak ground accelerations, station TAP22 (open circles), TAP37 (black circles), and TAP38 (crosses); and (b) 5% response spectra for station TAP22. The solid line denotes the average residuals (model bias); the thin lines show ±1 standard deviation limits; the dashed line shows distribution of the standard deviation versus the period.

obtained using 1D models (average values for SH- and SV-waves and for six incidence angles: 10, 20, 30, 40, 50 and 60°) and empirical ratios for the stations which are characterized by different thickness of Quaternary deposits and approximately the same character of the site response during deep and shallow earthquakes. It is seen that multilayered models reveal good agreement with empirical data, and the theoretical curves lay within ±1 standard deviation limits. Amplitudes on the amplification peaks depend on the impedance ratio between the basement (V_{S1} ρ_1) and the layer (V_{S2} ρ_2), and the quality factor $Q(f)$ combined with the layer thickness determines the amplification at high frequencies. Most probably, the difference between amplitudes of theoretical and empirical spectral ratios is caused by the discrepancy in accepted and real properties of the Quaternary deposits. The site response for stations located near the edge of the basin can be modeled accurately by the 1D model using single shallow and low impedance surface layer; complex multilayer 1D model is required to describe the site amplification for the stations located on the deep sediments. However, the 1D models fail to predict the spectral ratios for the sites located near subsurface topographic irregularities.

4. Ground motion modeling

The assessment of seismic hazard on the basis of ground motion attenuation relationships demands special studies to check whether the combination of source–path–site response models allow to calculate realistic "site and region-depending" strong motion estimations. The stochastic simulation technique introduced by Boore [10] was used to generate synthetic time histories of ground motion for a single earthquake. One of the most important parameters of used stochastic predictions is the duration model, because it is assumed that most (90%) of the spectral energy given by Eq. (1) is spread over a duration $\tau_{0.9}$ of the accelerogram. By comparing empirical and modeled peak amplitudes of ground acceleration, it has been found [20] that the duration model proposed by Wen and Yeh [21] in the following form

$$\tau_{0.9} = 0.430 \exp(0.504 M_L) \pm 2.749 \quad (8)$$

gives a better fit to the empirical data, and it was chosen as the most suitable for stochastic simulation in Taiwan area. PGA values were calculated for 28 earthquakes at station TAP22, for 16 earthquakes at station TAP37 and for 18 earthquakes at station TAP38 using recently obtained regional source scaling and attenuation models, and mean-amplitude site amplification function. The site response for station TAP22 is characterized by prominent amplification at intermediate frequencies that does not depend on the earthquake depth (see Fig. 2). The amplification function for station TAP37 reveals a broadband amplification and the response depends on the earthquake depth. The site response for station TAP38 also depends on the earthquake depth; however, it reveals a prominent peak for the amplification within a relatively narrow frequency band. Fig. 6a shows distribution of residuals Δ between modeled A_M and registered A_R (both horizontal components) maximum

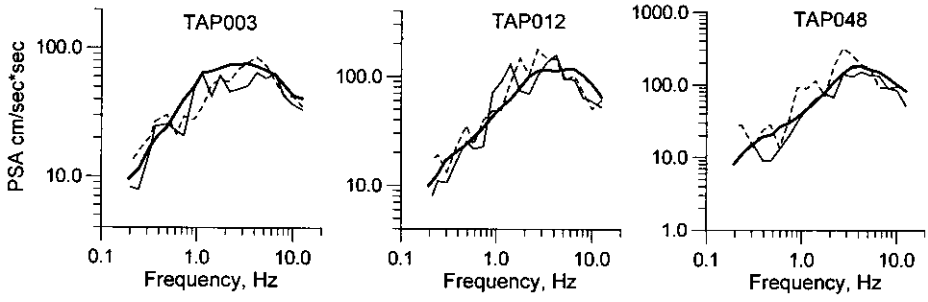

Fig. 7. Comparison of 5% damped response spectra (thin lines, solid and dashed lines denote N–S and E–W components, respectively) and spectra simulated using VHR spectra model and empirical site amplification functions (thick line, averaged from 40 simulations) for the event of 5 June 1994, $M = 6.2$.

amplitudes $\Delta = \log_{10} A_R - \log_{10} A_M$. It is seen that Wen and Yeh's duration model shows good agreement with empirical data. For this case the mean residual is 0.02 with standard deviation 0.15. To provide a quantitative measure of the accuracy of ground motion estimation using developed site–path–site response models, we estimate statistical characteristics of the residual Δ between modeled R_M and registered R_R (both horizontal components) response spectra ($\Delta = \log_{10} R_R - \log_{10} R_M$). For this purpose, as in the case of the PGA values comparison, 28 earthquakes registered at station TAP22, 16 earthquakes at station TAP37 and 18 earthquakes at station TAP38 were used. Fig. 6b shows the model bias (e.g. average residuals) along with ± 1 standard deviation. The results show little or no bias from low periods up to 1 s. For periods greater than 1 s, the observed spectra are, on an average, larger than the simulated ones due to the presence of ambient seismic noise [18]. At the same time, standard deviation does not increase greater than 0.3 log unit (average value 0.25) for the whole range of considered periods.

We also compared simulated and observed 5% damped response spectra for typical site conditions, namely: (a) deep Quaternary deposits (thickness more than 200 m), station TAP03; and (b) Quaternary deposits of intermediate thickness (about 150–200 m), station TAP12; shallow deposits (thickness less than 50 m), station TAP48 (Fig. 7). The $M = 6.2$ shallow ($H = 5$ km) earthquake of 5 June 1994 were used for the comparison. The simulated spectra essentially fit the observed data for considered site conditions.

5. Probabilistic seismic hazard assessment

The method used in this study is based on Cornell's [22] approach to probabilistic seismic hazard assessment which incorporates the influence of all potential sources of earthquakes and the activity rate assigned to them. It is assumed that earthquake occurrence is a stationary random process and the time, size and location of any earthquake are independent of the time, size and location of every previous earthquake. However, our approach and computational scheme differ from the classical ones and, therefore, we should describe the principal statements (see also Ref. [23]). We use a combination of so-called "fault" and "area-source" models. The possible earthquake sources are specified by geometry (in three dimensions) and a function describing area as a function of magnitude. At the same time, the earthquakes occur within the areas (source zones) characterized by maximum possible magnitude M_{max}. Instead of cumulative magnitude-recurrence model which determines number N of events with a magnitude m larger than M, we use alternative model and define N as the number of events with a magnitude $m = M \pm \delta m$. We also consider the probability distribution of hypocentral depth for earthquake sources.

For a given earthquake occurrence, the probability that a ground motion parameter X will not exceed a particular value x can be computed using the total probability theorem, that is

$$P[X \le x] = P[X \le x|Y]P[Y] \tag{9}$$

where Y is a vector of random variables (earthquake of magnitude M and distance R) that influence X. Assuming that M and R are independent, the probability of non-exceedance can be written as

$$P[X \le x] = \int\int P[X \le x|m, r] f_M(m) f(r) \mathrm{d}m\, \mathrm{d}r \tag{10}$$

where $P[X \le x|m, r]$ is obtained from the predictive relationship and $f_M(m)$ and $f(r)$ are the probability density functions for magnitude and distance, respectively. When performing PSHA using classical scheme, it is necessary to determine the temporal distributions of earthquake recurrence and source-to-site probability distributions for source zones. In our scheme we do not use the probability density function $f_M(m)$ and $f(r)$, and consider every potential earthquake as a separate event. Thus, Eq. (9) may be rewritten as

$$P[X \le x] = P[X \le x|Y(m_1, r_1)] \times P[X \le x|Y(m_2, r_2)] \times \cdots \times P[X \le x|Y(m_N, r_N)] \tag{11}$$

where $Y(m_i, r_i)$ is the potential earthquake with magnitude $M_{min} \le m \le M_{max}$ and distance $R_{min} \le r \le R_{max}$

Let us assume that the level of seismic hazard is controlled by the total influence of all earthquakes that may occur in the region under study, and also that the characteristics of ground motion expected during an earthquake of given M and R are log-normally distributed with standard deviation σ_x. Then, for a single earthquake of magnitude $M = m$ and focus depth $H = h$ occurring at distance $R = r$, the probability that ground motion parameter will not exceed a given value may be estimated as follows:

$$P_{N(M=m;R=r;H=h)=1}[X \le x] = \frac{1}{\sigma_x \sqrt{2\pi}} \int_{x_{min}}^{x} \exp((x-a)^2/2\sigma_x^2)\mathrm{d}x \tag{12}$$

where a is the mean value of $\log_{10} X$ (X — ground motion characteristic) for an earthquake of given M and R; and x_{min} is of sufficiently small value ($x_{min} \approx a - 5\sigma_x$). Sources of ground motion parameter uncertainty are inherent randomness in the source rupture, the characteristics of the wave-propagation path, and variability in the subsoil and geological conditions. Therefore, strictly speaking, standard deviation is a function of magnitude, distance, soil condition and oscillator frequency.

Eq. (12) allows us to estimate the seismic effect due to a single earthquake of given characteristics (M, R and H). If the depth of possible earthquake source may be specified

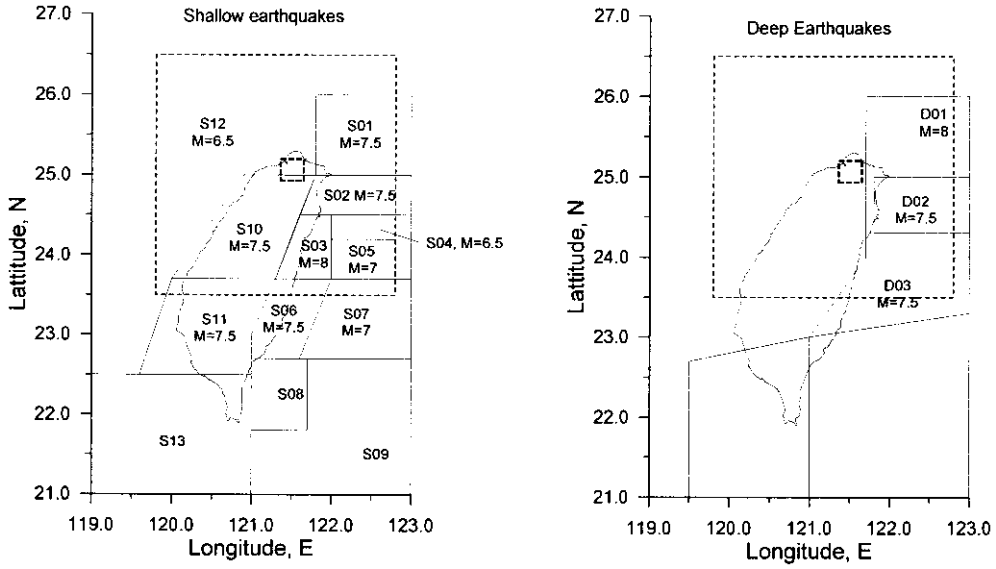

Fig. 8. Zoning schemes with maximum magnitudes M for shallow and deep seismicity (after Loh and Jean [24]. The thin dashed lines show the region used for seismic hazard calculation, the thick dashed lines show the Taipei basin.

within a certain interval ($H_{\min} \le h \le H_{\max}$), then

$$P_{N(M=m;R=r)=1}[X \le x] = \sum_{H_{\min}}^{H_{\max}} \{P_{N(M=m;R=r;H=h)=1}[X \le x] P_{M=m}[H = h]\} \quad (13)$$

where $P_{M=m}[H = h]$ is the probability that the depth (H) of the earthquake source equals h.

To consider earthquake occurrence, it is necessary to substitute the probability distribution function for a single ($N = 1$) earthquake using the probability distribution function for at least one ($N \ge 1$) earthquake of given M and R.

$$P_{N(M=m;R=r)\ge 1}[X \le x] = \sum_{N=1}^{n} \{(P_{N(M=m;R=r)=1}[X \le x])^n P_{M=m}[N = n]\} \quad (14)$$

where $P_{M=m}[N = n]$ is the probability that n earthquakes of magnitude $M = m$ will occur during specified time period t assuming a Poissonian distribution of the earthquakes. The probability is calculated as

$$P_{M=m}[N = n] = \frac{(\lambda_m t)^n}{n!} \exp(-\lambda_m t) \quad (15)$$

where λ_m is the average number of earthquakes of $M = m$ per unit time and n is the expected number of the earthquakes.

Considering all earthquakes of $M_{\min} \le m \le M_{\max}$ that may produce significant effect at given distance $R = r$ and assuming their independence, we have the following

$$P_{N(R=r)\ge 1}[X \le x] = \prod_{M_{\min}}^{M_{\max}} P_{N(M=m;R=r)\ge 1}[X \le x] \quad (16)$$

The final expression that takes into account that all distances from $r_{\min} \le R \le r_{\max}$ is as follows:

$$P_{N\ge 1}[X \le x] = \prod_{r=r_{\min}}^{r=r_{\max}} P_{N(R=r)\ge 1}[X \le x] \quad (17)$$

Here $r_{\max}$ is the maximum distance at which the earthquake of $M = m$ may produce significant effect.

The average return period T of ground motion parameter X exceeding the given value x may be estimated from the equation

$$P_{N=0}[X > x] = \exp(-\gamma_x T) = P_{N\ge 1}[X < x] \quad (18)$$

assuming a Poissonian distribution of the events (ground motion exceedance) with mean rate γ_x.

We based the seismic hazard calculations on the Fourier amplitude spectra (FAS) parameter X in Eq. (12), and we include in the calculations all possible sources of earthquakes that may occur within a region surrounding the site. The size of the region is chosen assuming that the greatest earthquake ($M = M_{\max}$), occurring at the largest distance (within the region), will not produce a significant effect on the observation site. The procedure used a system of grid points (elementary segments) with $10 \times 10\ \mathrm{km}^2$ spacing. Possible earthquakes will occur within a volume of the Earth's crust, and their hypocenters are located under the central points of the grid. Every elementary area is characterized by the following parameters: (1) minimum ($M_{\min}$) and maximum ($M_{\max}$) magnitudes of possible earthquakes which will occur underneath the segment; (2) probability distribution of hypocentral depth for earthquake sources of $M_{\min} \le M \le M_{\max}$; (3) rates of earthquake recurrence per unit time; and (4) source (near-field) Fourier acceleration spectra.

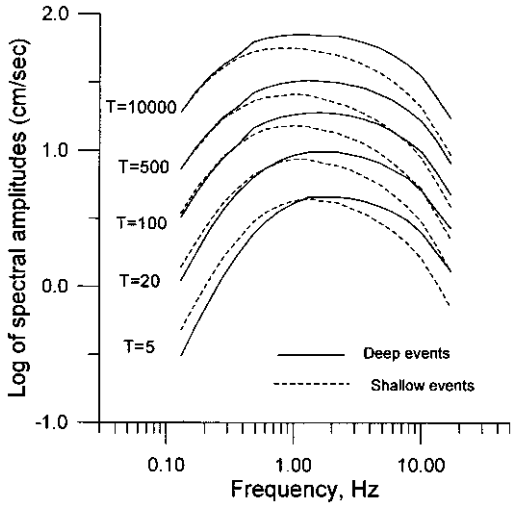

Fig. 9. Uniform hazard Fourier spectra (acceleration, rock site) estimated for different return periods T (probability of exceedance in specified exposure time) using data for shallow and deep seismicity.

The earthquake sources are modeled as ellipsoidal planes, and the rupture area depends on the magnitude. The uncertainty in the geometry of seismic sources is considered using the following: every source is characterized by the sets of the strike and dip angles (3–5 values with correspondent weights), and the distance between the site and the nearest point of the source is calculated as the averaged value.

Fig. 8 shows seismogenic zoning schemes for shallow (hypocentral depth $H \leq 35$ km) and deep ($H > 35$ km) seismicity [24]. Calculations were performed for the central point of the Taipei basin (thick dashed lines), taking into account possible earthquakes in the surrounding region (thin dashed lines). The earthquake occurrence models for every zone were determined, using regional catalogues, on the basis of frequently used magnitude–frequency relationship

$$\log_{10} N_m = a - bm \tag{19}$$

where a and b are the regional constants and N_m is the number of earthquakes of magnitude $m \pm \delta m$ per unit time and unit area. When estimating the recurrence relationships, we used the regional catalogue data: earthquake of $M_L > 3$ which occurred between January 1973 and December 1998. Prior to the installation of the telemetric seismographic network in Taiwan in 1972, the records of earthquakes of significant magnitudes may not be totally complete. The 26 year period of observation is too short to determine recurrence parameters, especially for earthquakes of large magnitudes. Therefore, we also used a second data set: earthquakes which occurred between January 1900 and December 1998 to verify the recurrence of large events. We determined the parameters of the recurrence relationships (a and b) for $M > 5.5$ using both data sets.

Fig. 9 shows uniform hazard Fourier spectra (UHFS) of ground acceleration estimated for the condition of "very hard rock" site for central part of the Taipei basin. These estimations have been made assuming standard deviation $\sigma_x = 0.3$ log units (Eq. (12)) of the spectra. It is seen that the UHFS levels for the deep and shallow seismicity are approximately equal for the low ($f < 1$–2 Hz) frequencies, and the spectral amplitudes for the deep seismicity are somewhat higher for the frequencies more than 2 Hz. This phenomenon is explained by applying different attenuation models for the shallow and deep earthquakes. Inelastic attenuation of spectral amplitudes in the model accepted is described by quality factor Q that is usually written in the form $Q = Q_0 f^n$. The greater the factor Q the lesser the decrease of the spectral amplitudes with distance. We used $Q = 225 f^{1.1}$ for the deep events and $Q = 125 f^{0.8}$ for the shallow events. The last model causes more rapid attenuation of the spectral energy at the high frequencies for shallow events as compared with those for deep earthquakes.

To make the results of probabilistic seismic hazard assessment clearer and more useful for engineering purposes, the so-called *deaggregation* procedure is used [25–29]. The hazard is represented by a single or several earthquakes of certain magnitude M and distance R (so-called dominant earthquakes) that determine the motion in a given frequency range. Ground motion parameters for engineering purposes can be obtained (generated or selected) for these (M, R) pairs. Generally, a single dominant earthquake will not reasonably represent the UHS, and multiple design events should be considered. In this study, the dominant earthquakes, determined for a given return period (probability of exceedance), are used to generate ground motion time series for the whole frequency band studied on the basis of UHFS. These time series (uniform hazard accelerograms) do not represent ground motion for a single earthquake, but may be considered as a combination

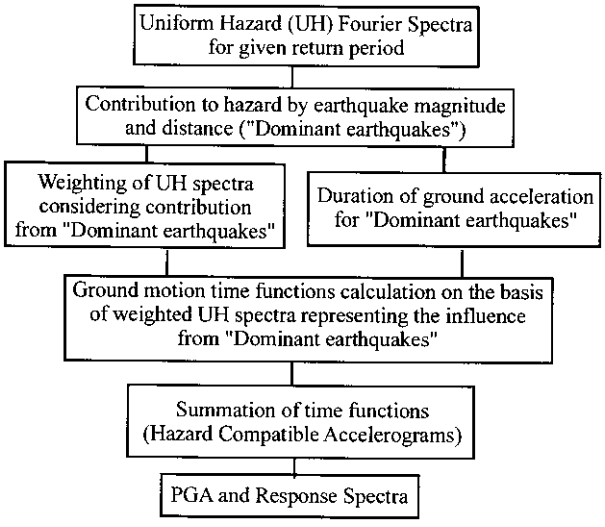

Fig. 10. Scheme of probabilistic seismic hazard assessment on the basis of the Fourier amplitude spectra.

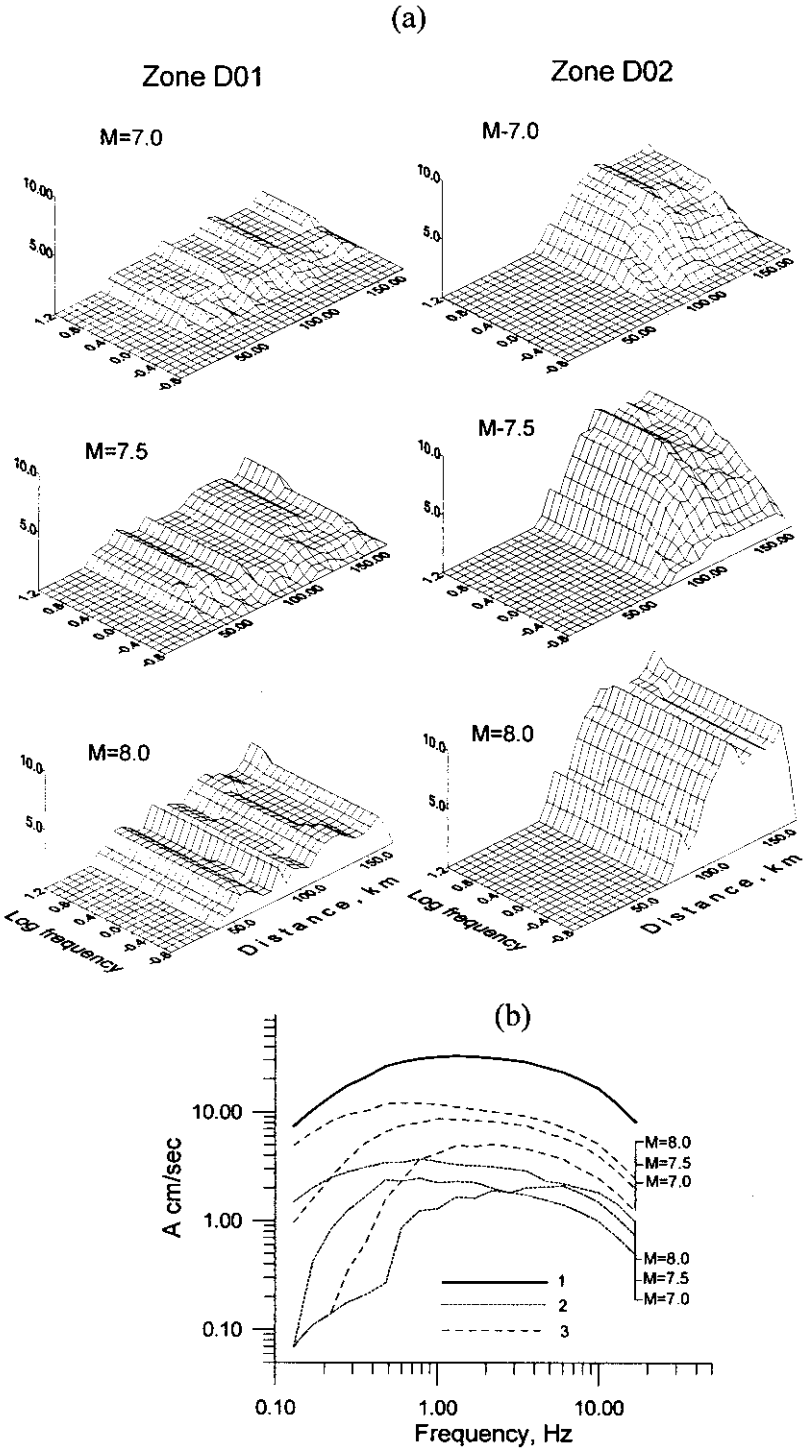

Fig. 11. (a) Relative contribution (percentage/10) to the Fourier spectra hazard (return period 475 year) by earthquakes of magnitudes M (deep seismicity); and (b) uniform hazard Fourier spectrum (1) of ground acceleration (deep seismicity, hard rock, return period $T = 475$ year) and "weighted" spectra representing the contribution from dominant earthquakes of magnitude M in the zones D01 (2) and D02 (3).

of the motion components in the chosen frequency range, parameters of which (spectral amplitudes) will not be exceeded with a certain probability in a specified time period (e.g. 10% in 50 year). Actually, when the engineering design requires the mutual consideration of various frequencies, say 1, 3 and 10 Hz, the vibrations at which are contributed by different events, the use of uniform hazard accelerograms for dynamic analysis could be a source of additional conservatism in engineering decisions, because it implies, simultaneously, the influence from several earthquakes, for example a small, nearby earthquake and a large, distant one. PGA and response spectra are

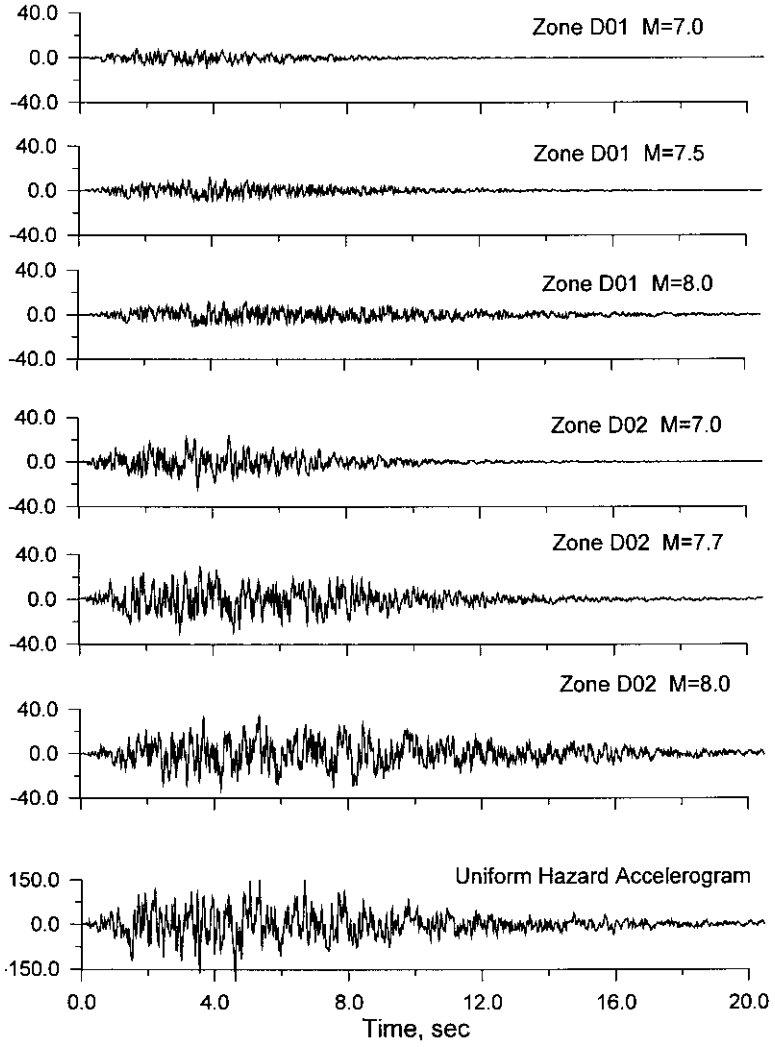

Fig. 12. Ground motion time functions (acceleration, cm/s^2), which represent influence from dominant earthquakes and uniform hazard accelerogram (hard rock, return period $T = 475$ year).

calculated directly form these accelerograms, and they are the hazard-compatible estimations. On the other hand, since we used the region- and site-dependent Fourier spectra for the calculation (Eq. (12)), it is possible to estimate "region and site and return period-dependent" design input ground motion parameters. The scheme of this approach is shown in Fig. 10.

It can be seen from Eqs. (16) and (17) that the total probability of ground motion parameter X (Fourier amplitude spectrum of ground acceleration) not to be exceeded is determined by multiplication of the probability functions for different M and R values. Therefore, it is possible to determine the influence from every (M, R) event, and the "dominant earthquake" for a given return period should be characterized by the largest value $(1.0 - P_{(M=m;R=r)}[X \leq x])$. Note that the distribution for the earthquake depths and occurrence of the events have been already taken into consideration. The value x, controlling the contribution of (M, R) pairs, is determined using Eq. (18) for a given return period T (probability of exceedance in a specified exposure time).

Fig. 11 shows the relative contribution to Fourier spectra hazard (return period $T = 475$ year) by deep earthquakes of magnitude M and distance R at different frequencies. Return period 475 year (annual probability of exceedance 1/475; 10% probability of being exceeded during 50 year) is a standard value used for ordinary buildings. The hazard from deep earthquakes is mainly determined by earthquakes in the zone D02, and the contribution depends of the ground motion frequency. The long-period motion is determined by large ($M = 8.0$) earthquakes that may occur in the zone D02 at distances $R > 100$ km from the studied area. Earthquakes of $M < 8$ significantly contribute to hazard in high-frequency domain. In this case ($T = 475$ year, deep seismicity) it is possible to choose the following "dominant earthquakes" for both the D01 and D02 zones: (a) $M = 7.0$, $R = 120$–140 km; (b) $M = 7.5$, $R = 120$–140 km; and (c) $M = 8.0$, $R = 120$–140 km. The UHFS has been

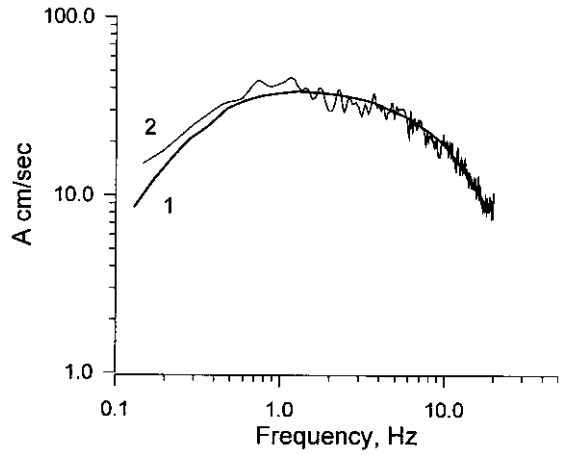

Fig. 13. Comparison of uniform hazard Fourier spectrum (1) (hard rock, return period $T = 475$ year) and the smoothed spectrum (averaged from a set of 40 time histories) of uniform hazard accelerogram (2).

Table 1
Peak ground accelerations (cm/sec^2) estimated for various return period for different site conditions in the Taipei basin

Site condition	Return period (year)		
	5	50	500
Shallow seismicity			
Hard rock	20	50	100
Average soil	40	90	220
Deep seismicity			
Hard rock	25	75	180
Average soil	50	130	300
St. TAP03	–	–	170
St. TAP12	–	–	230
St. TAP22	–	–	450

weighted taking into account the relative contribution from "dominant earthquakes" to produce "characteristic" spectra that represent influence from "dominant earthquakes". Fig. 11b shows UHFS and "weighted" spectra. Acceleration time functions that have been generated using the stochastic approach on the basis of the "weighted" spectra are shown in Fig. 12. The ground motion duration values were estimated for "dominant earthquakes" using the regional relationship proposed by Wen and Yeh [21] (Eq. (8)).

Summation of the time functions, which are calculated from the "weighted" spectra, produces UHFS-compatible accelerogram or uniform hazard accelerograms. The summed amplitude should be multiplied by $N^{1/2}$ due to the incoherence of summation [30], where N is the number of "characteristic accelerograms" (or "dominant earthquakes"). Fig. 13 compares averaged (from 40 simulations) and smoothed spectrum of uniform hazard accelerograms with target UHFS and shows that the two match reasonably well for all frequencies. When a set of uniform hazard accelerograms is calculated, the maximum amplitudes averaged from the set produce so-called PGA hazard and UHS may be evaluated.

In order to obtain "site-dependent" estimations in the Taipei basin, the UHFS were calculated for every station of the TSMIP network, for which the site response characteristics were studied [18]. "Hazard-compatible" PGA values and response spectra were estimated using the described scheme for these sites. Fig. 14 shows the schemes of PGA distribution along the Taipei basin, which were calculated for return period 475 year for shallow and deep seismicity. The schemes are compared with the variation of maximum amplitudes observed during two large and distant events: 5 June 1994, $M_L = 6.4$, $H = 5$ km, and 25 June 1995, $M_L = 6.5$, $H = 40$ km. Of course, we should not

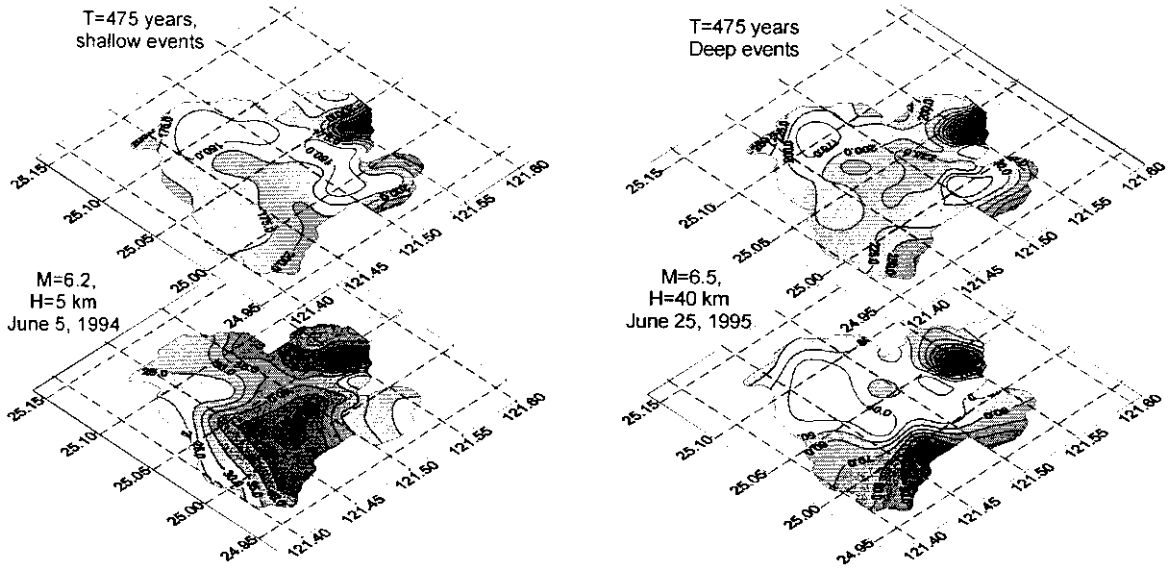

Fig. 14. Comparison of the PGA (cm/sec^2) distribution along the Taipei basin obtained from the hazard calculations for shallow and deep events, and real earthquakes.

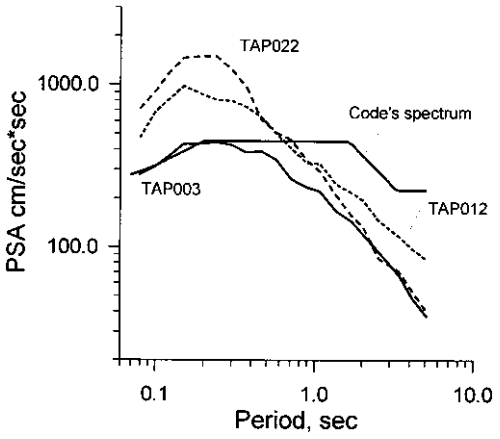

Fig. 15. Comparison of uniform hazard response spectra estimated for different soil conditions (the Taipei basin, return period $T = 475$ year), and design response spectrum defined in building code for the Taipei basin (CSSE [8]).

expect an excellent coincidence between the PGA distribution patterns during the real earthquakes and those obtained by seismic hazard calculations. The averaged spectral ratios [18] have been used in the hazard assessment, therefore the "site-dependent" hazard estimations are believed to reflect general features of ground motion parameter distribution in the studied area. However, it can be seen that the calculated PGA patterns for both shallow and deep seismicity generally agree with the empirical ones and they reveal the lowest PGAs in the northern and southeastern parts of the Taipei basin. The PGA values increase when approaching the north and south edges, and the southeastern part of the basin is characterized by the highest PGA values.

Table 1 lists the PGA values, which were obtained from the uniform hazard accelerograms for different return periods. As a rule, a 10% probability of exceedance in 50 year applies to most building codes for ordinary buildings. It corresponds to 1/475 annual probability of exceedance (or return period $T = 475$ year). For buildings classified within other importance categories, different return periods (annual probability of exceedance) may be applied. Reference return periods from about 100 to 1000 year are generally applicable to electric system components, and larger return periods (up to 10 000 year) are applicable to dams [31]. At the same time, small return periods (less than 50–100 year) may also be useful for estimation of the hazard assessment reliability by comparing with available ground motion recordings. It is necessary to note that our results of seismic hazard estimation in terms of peak acceleration obtained in this study are in good agreement with results of hazard analyses obtained recently [24] on the basis of regional PGA attenuation relationships for averaged soil sites (220–240 cm/s^2 for return period of 475 year). PGA values may vary significantly depending on the site conditions (the thickness of Quaternary deposits), and this phenomenon has been observed during recent earthquakes [5–7].

Let us consider the typical soil profiles for the Taipei basin, namely: station TAP03 — deep Quaternary deposits (thickness greater than 250 m, near the deepest part of the Taipei basin); stations TAP12 — Quaternary deposits of intermediate thickness (about 150–200 m, central part of the basin); station TAP22 — shallow deposits (thickness less than 50 m, the site is situated near the basin edge). The UHS (5% damping, return period $T =$ 475 year, deep seismicity), which was estimated for the considered site conditions in the Taipei basin, using empirical site amplification functions, are shown in Fig. 15. The amplitudes of the spectrum for deep Quaternary deposits (station TAP03) are constantly lesser than those estimated for the deposits of intermediate thickness (station TAP12). The shallow-soil site near the edge of the Taipei basin (TAP22) is characterized by the largest low-period ($T < 0.3$–0.4 s) level of the response spectra. The difference between low-period amplitudes of the response spectra for the sites situated on the deepest part of the basin and the basin edge may exceed a factor of 3, and it decreases with increasing of ground motion period. The figure compares the UH site-dependent response spectra and the building code's design response spectrum for the Taipei basin [8], calculated as ground motion period-dependent seismic force coefficient C multiplied by seismic zone factor ($0.23g$ for the Taipei area). As a matter of fact, the code-provided design spectrum of the Taipei basin in long-period range was developed using the recorded data of the 15 November 1986 earthquake ($M = 6.8$, $H = 10$ km, $R > 100$ km). It is seen that, in short-period range, the code-provided spectrum may be considered as a proper one only for deep Quaternary deposits. At the same time, for periods more than 0.8–1.0 s the code's design spectrum is characterized by higher amplitudes that the UHS. Due to the presence of long-period ambient noise, the analysis of site response has been limited by the frequencies less than 0.4–0.5 Hz. Therefore, the UHS for periods more than 2 s may be underestimated. It has also been shown that the difference between averaged spectral ratios for shallow and deep earthquakes may exceed a factor of 1.5 both in low- and high-frequency domain. When calculating the UHS for different site conditions, we used the mean amplitude amplification functions both for deep and shallow events.

6. Conclusions

An integrated approach for evaluating "site-dependent" seismic hazard in terms of ground motion parameters used for engineering purposes is presented in this paper. Empirical models for source, propagation path and site effects, which were obtained on the basis of the collection of ground motion recordings of small to moderate ($4.5 \leq M_L \leq 6.5$) earthquakes in the Taiwan area were used in the hazard calculation. The results of the ground motion data

analysis reveal that the acceleration spectra of most significant part of the records, starting from S-wave arrival, can be modeled accurately by the Brune's ω-squared source model with magnitude-dependent stress parameter $\Delta\sigma$, that should be determined using recently proposed regional relationships between local magnitude (M_L) and seismic moment (M_0) and between M_0 and $\Delta\sigma$. The anelastic attenuation Q of spectral amplitudes with distance may be described as $Q = 225f^{1.1}$ for deep (depth greater than 35 km) and $Q = 125f^{0.8}$ shallow earthquakes. Effects of local site response are considered by means of empirical soil/bedrock spectral ratios calculated for the sites in the Taipei basin as ratio between spectra of actual earthquake records and those modeled for hypothetical "very hard rock" site.

The results of the simulation demonstrate that this combination of source, path and site response models provides an accurate prediction of "site and region-dependent" ground motion parameters for the Taipei basin. The standard deviation of variance between the observed and computed maximum accelerations and response spectra does not exceed 0.3 log units. The models were used in probabilistic seismic hazard assessment for the Taipei basin. The estimations of "site and region-dependent" PGA for return period 475 year (10% of exceedance in 50 year), that were obtained using the proposed approach, show good agreement with the data estimated independently. This suggests that our estimations may be used as a reliable basis for building code provisions and engineering decisions. The amplitudes of the UHS strictly depend on the local soil conditions, and one single building code is not adequate for the whole basin area. The proposed scheme can be used as basis for probabilistic ("return period-dependent") microzonation in terms of engineering ground motion parameters.

There are some simplified assumptions both in input data and in calculation schemes. For example, the Poisson-process model was used to describe the earthquake occurrence; a simple point-source ω-squared model was used for the calculation of spectral amplitudes near the extended source; a linear model of soil response has been used for weak and strong, distant and nearby events; and a generalized envelope function was used in ground motion generation. But the general scheme of the approach can be improved as new and more complete data appear.

The results of seismic hazard estimation that take into account the local soil conditions reveal the necessity of detailed study of the site amplification function variability with respect the earthquake source depth, as well as the study of the site response in the low-frequency (below 1 Hz) domain. It is necessary to note that the characteristics of local site response in the Taipei basin were studied using the records from earthquakes located to the Southeast of the basin. The recent strong Chi-Chi earthquake of 21 September 1999 ($M_L = 7.3$) produced the basis for studying the influence of azimuthal direction of incident excitation on the basin response. These are the topics of future research.

References

[1] Kuo K-W, Shin T-C, Wen K-L. Taiwan strong motion instrumentation program (TSMIP) and preliminary analysis of site effects in Taipei basin from strong motion data. In: Cheng F-Y, Cheu MS, editors. Urban disaster mitigation: the role of engineering and technology, Amsterdam: Elsevier, 1995. p. 47–62.

[2] Aki K. Local site effect on strong ground motion. In: Von Thun JL, editor. Recent advances in ground-motion evaluation, Proceedings of Earthquake Engineering and Soil Dynamics, vol. II. New York: American Society for Civil Engineers, 1988. p. 103–55.

[3] Aki K, Irikura K. Characterization and mapping of earthquake shaking for seismic zonation. In Fourth International Conference on Seismic Zonation. Proceedings of EERI, 1991, p. 61–110.

[4] Bard PY. Effects of surface geology on ground motion: recent results and remaining issues. Proceedings of the 10th European Conference on Earthquake Engineering, Rotterdam: Balkema, 1995. p. 305–23.

[5] Wen K-L, Peng H-Y, Liu L-F, Shin T-C. Basin effect analysis from a dense strong motion observation network. Earthquake Engng Struct Dyn 1995;24:1069–83.

[6] Loh C-H, Hwang J-Y, Shin T-C. Observed variation of earthquake motion across a basin, Taipei city. Earthquake Spectra 1998;14(1):115–33.

[7] Wen K-L, Peng H-Y. Site effect analysis in the Taipei basin: results from TSMIP network data. Terrestrial Atmos Ocean Sci 1998;9:691–704.

[8] Chinese Society of Structural Engineers. Seismic Design Codes for Building. Report CSSE 84-03B.

[9] Sokolov V, Loh C-H, Wen K-L. Empirical model for estimating Fourier amplitude spectra of ground acceleration in Taiwan region. Earthquake Engng Struct Dyn 2000;29:339–57.

[10] Boore DM. Stochastic simulation of high frequency ground motion based on seismological model of the radiated spectra. Bull Seismol Soc Am 1983;73:1865–94.

[11] Brune JN. Tectonic stress and the spectra of seismic shear waves from the earthquakes. J Geophys Res 1970;75:4997–5009.

[12] Anderson J, Hough S. A model for the shape of the Fourier amplitude spectrum of acceleration at high frequencies. Bull Seismol Soc Am 1984;74:1969–93.

[13] Li C, Chiu H-C. A simple method to estimate the seismic moment from seismograms. Proc Geol Soc Chin 1989;32:197–207.

[14] Tsai C-CP. Relationships of seismic source scaling in the Taiwan region. Terrestrial Atmos Ocean Sci 1997;8:49–68.

[15] Boore DM, Atkinson GM. Stochastic prediction of ground motion and spectral response parameters at hard rock sites in eastern North America. Bull Seismol Soc Am 1987;77:440–67.

[16] Boore DM, Joyner WB. Site amplification for generic rock sites. Bull Seismol Soc Am 1997;87:327–41.

[17] Atkinson GM, Silva W. Stochastic modeling of California ground motions. Bull Seismol Soc Am 2000;90:255–74.

[18] Sokolov V, Loh C-H, Wen K-L. Empirical study of sediment-filled basin response: the case of Taipei city. Earthquake Spectra 2000;16:681–707.

[19] Sokolov V. Rough estimation of site response using earthquake ground motion records. Proceedings of the Second International Symposium on the Effects of Surface Geology on Seismic Motion, Yokohama, Japan, 1–3 December 1998, Rotterdam: Balkema, 1998. p. 517–22.

[20] Sokolov V, Loh C-H, Wen K-L. Empirical models for estimating design input ground motions in Taiwan region. In Proceedings of the International Workshop on Mitigation of Seismic Effects on Transportation Structures, Taipei, Taiwan, 12–14 July 1999. p.154–63.

[21] Wen K-L, Yeh Y-T. Characteristics of strong motion durations in the SMART1 array area. Terrestrial Atmos Ocean Sci 1991;2:187–201.

[22] Cornell CA. Engineering seismic risk analysis. Bull Seismol Soc Am 1968;58:1583–606.
[23] Sokolov V. Hazard-consistent ground motions: generation on the basis of uniform hazard Fourier spectra. Bull Seismol Soc Am 2000;90:1010–27.
[24] Loh C-H, Jean W-Y. Seismic zoning on ground motions in Taiwan area. In Fourth International Conference on Soil Mechanics and Foundation Engineering, September 1997. p. 71–9.
[25] Chapman MC. A probabilistic approach to ground-motion selection for engineering design. Bull Seismol Soc Am 1995;85:837–42.
[26] McGuire RK. Probabilistic seismic hazard analysis and design earthquakes: closing the loop. Bull Seismol Soc Am 1995;85:1275–84.
[27] Cramer CH, Petersen DM. Predominant seismic source distance and magnitude maps for Los Angeles, Orange, and Ventura counties, California. Bull Seismol Soc Am 1996;86:1645–59.
[28] Harmsen S, Perkins D, Frankel A. Deaggregation of probabilistic ground motions in the central and eastern United States. Bull Seismol Soc Am 1999;89:1–13.
[29] Bazzuro P, Cornell CA. Disaggregation of seismic hazard. Bull Seismol Soc Am 1999;89:501–20.
[30] Joyner WB, Boore DM. On simulating large earthquakes by Green's function addition of smaller earthquakes. In: Das S, Boatwright J, Scholz C, editors. Fifth Maurice Ewing Symposium on Earthquake Source Mechanics, American Geophysical Union, 1986. p. 269–74.
[31] Little TE, Meidal KM. Ground motion studies for a west cost electric utility. In Proceedings of the Fifth US National Conference on Earthquake Engineering, Chicago, vol. III, 10–14 July 1994. p. 261–70.